

Effects of cesium ion-implantation on mechanical and electrical properties of organosilicate low-k films

W. Li, D. Pei, X. Guo, M. K. Cheng, S. Lee, Q. Lin, S. W. King, and J. L. Shoet

Citation: [Applied Physics Letters](#) **108**, 202901 (2016); doi: 10.1063/1.4950717

View online: <http://dx.doi.org/10.1063/1.4950717>

View Table of Contents: <http://scitation.aip.org/content/aip/journal/apl/108/20?ver=pdfcov>

Published by the [AIP Publishing](#)

Articles you may be interested in

[Characterization and versatile applications of low hydrogen content SiOCN grown by plasma-enhanced chemical vapor deposition](#)

J. Appl. Phys. **116**, 104902 (2014); 10.1063/1.4894843

[Effects of plasma and vacuum-ultraviolet exposure on the mechanical properties of low-k porous organosilicate glass](#)

J. Appl. Phys. **116**, 044103 (2014); 10.1063/1.4891501

[Effect of water uptake on the fracture behavior of low-k organosilicate glass](#)

J. Vac. Sci. Technol. A **32**, 031512 (2014); 10.1116/1.4871680

[The effect of water uptake on the mechanical properties of low-k organosilicate glass](#)

J. Appl. Phys. **114**, 084103 (2013); 10.1063/1.4817917

[Compositional effects on electrical and mechanical properties in carbon-doped oxide dielectric films: Application of Fourier-transform infrared spectroscopy](#)

J. Vac. Sci. Technol. B **22**, 196 (2004); 10.1116/1.1640401

A promotional banner for Applied Physics Reviews. On the left is a thumbnail of a journal cover titled 'AIP Applied Physics Reviews' featuring a diagram of a layered structure. The main text reads 'NEW Special Topic Sections' in large white letters. Below this, it says 'NOW ONLINE' in yellow, followed by 'Lithium Niobate Properties and Applications: Reviews of Emerging Trends' in white. The AIP Applied Physics Reviews logo is in the bottom right corner.

NEW Special Topic Sections

NOW ONLINE
Lithium Niobate Properties and Applications:
Reviews of Emerging Trends

AIP Applied Physics
Reviews

Effects of cesium ion-implantation on mechanical and electrical properties of organosilicate low- k films

W. Li,¹ D. Pei,¹ X. Guo,¹ M. K. Cheng,¹ S. Lee,¹ Q. Lin,² S. W. King,³ and J. L. Shohet¹

¹Plasma Processing and Technology Laboratory, Department of Electrical and Computer Engineering, University of Wisconsin-Madison, Madison, Wisconsin 53706, USA

²IBM T.J. Watson Research Center, Yorktown Heights, New York 10598, USA

³Intel Corporation, Hillsboro, Oregon 97124, USA

(Received 16 March 2016; accepted 4 May 2016; published online 17 May 2016)

The effects of cesium (Cs) ion-implantation on uncured plasma-enhanced chemical-vapor-deposited organosilicate low dielectric constant (low- k) (SiCOH) films have been investigated and compared with an ultraviolet (UV) cured film. The mechanical properties, including the elastic modulus and hardness, of the SiCOH low- k films are improved by up to 30% with Cs implantation, and further up to 52% after annealing at 400 °C in a N₂ ambient for 1 h. These improvements are either comparable to or better than the effects of UV-curing. They are attributed to an enhancement of the Si-O-Si network structure. The k -value of the SiCOH films increased slightly after Cs implantation, and increased further after annealing. These increases are attributed to two carbon-loss mechanisms, i.e., the carbon loss due to Si-CH₃ bond breakage from implanted Cs ions, and the carbon loss due to oxidation during the annealing. The time-zero dielectric breakdown strength was improved after the Cs implantation and the annealing, and was better than the UV-cured sample. These results indicate that Cs ion implantation could be a supplement to or a substitution for the currently used UV curing method for processing SiCOH low- k films. *Published by AIP Publishing.*

[<http://dx.doi.org/10.1063/1.4950717>]

Low dielectric constant (low- k) dielectrics are necessary to meet the performance and power consumption requirements of modern integrated circuits. Typically, these low- k dielectrics are organosilicate glasses. They are generally made of silicon (Si), carbon (C), oxygen (O), and hydrogen (H), which are called SiCOH, SiOCH, or SiOC:H.¹ To lower the value of k even further, sacrificial components, called porogens, are introduced and subsequently removed to form porous ultra-low- k dielectrics.^{2,3} Unfortunately, the introduction of pores significantly weakens the mechanical properties of the resultant porous dielectric and renders it susceptible to process-induced damage.^{2,4} As a result, such porous low- k dielectrics are extremely difficult to work with and pose significant challenges to continued scaling of integrated circuits.^{5,6}

Recent work in Japan⁷ demonstrated surprising improvements of the electrical properties, mechanical properties, and reliability of porous silica films with the addition of a cesium (Cs) salt during the synthesis of porous low- k films using a wet method. That is, adding Cs, although it appears to be counter-intuitive, makes the dielectric better!

In contrast to the aforementioned porous-silica film being formed with wet chemistry, SiCOH as a mainstream interlayer dielectric (ILD) can only be prepared with plasma-enhanced chemical-vapor deposition (PECVD) in order to be integrated with other processes.² At present, curing SiCOH using ultraviolet (UV) radiation offers some improvement in mechanical properties.^{8,9} However, there are tradeoffs. For example, after the UV exposure beyond what is required to remove the porogens, the k -value begins to increase. In addition, carbon loss, which results in an increase in defect concentration, also occurs simultaneously.^{10–12}

In this work, the effects of a “dry” Cs ion-implantation in SiCOH are investigated. The goal is to determine whether

the advantages previously obtained using wet chemistry could be obtained using Cs ion-implantation, thus being a potential supplement to or even a substitution for the incumbent UV curing method.

Two types of nonporous SiCOH low- k films deposited on (100) Si substrates with PECVD were used in this work: One set of films was uncured and the other was UV cured.² Neither of these two films had porogens involved in their forming process. Three uncured film samples were implanted with Cs ions under three different conditions. The UV-cured film was not implanted, but used as a comparison. The film properties and implantation conditions are summarized in Table I. Note that unimplanted samples (pristine) are labeled with letters A and B, where sample A is uncured and sample B is UV cured. The implanted samples are labeled as 1 to 3 with increasing Cs dose. In all the subsequent tables and figures, initials P, I, and IA indicate pristine, as implanted but not annealed, and implanted and annealed samples, respectively. The Cs doses were chosen such that the relative atomic concentrations in the low- k film varied from 20 to 200 ppm, assuming a uniform Cs distribution within the film. The ion-implantation energy was chosen to be 100 keV, based on a TRIM-code simulation.¹³ The simulation predicted that 100-keV Cs ions have a projected range between 100 and 110 nm. This range is approximately in the center of the film. All the implanted samples were eventually annealed in the atmospheric-pressure nitrogen ambient for 1 h at 400 °C, in order to redistribute the Cs atoms more uniformly within the film.

Ellipsometry was used to measure the film's thickness after each step of the procedure. Figure 1 shows the results. It can be seen that all the implanted films shrank slightly after implantation, and shrank even more after annealing.

TABLE I. Properties of pristine films and Cs ion-implantation conditions.

Film type	Thickness (nm)	Nominal k -value	Sample label	Cs ion dose (ions/cm ²)	Cs ion energy (keV)
Uncured	233.1	3.2	Sample A	N.A.	N.A.
Uncured	234.0	3.2	Sample 1	1×10^{13}	100
Uncured	231.9	3.2	Sample 2	5×10^{13}	100
Uncured	233.4	3.2	Sample 3	1×10^{14}	100
UV-cured	211.4	3.2	Sample B	N.A.	N.A.

This matches the observations in the previous work using the wet chemistry.⁷

Nanoindentation was used to measure the elastic modulus and hardness of the films. Details of this technique can be found in a previous publication.¹⁴ Figure 2 shows the results. The horizontal axis, h , is defined as

$$h = \frac{\sqrt{\text{contact area}}}{\text{film thickness}},$$

where the contact area is the area of the indenter tip actually in contact with the film; h is the dimensionless. This provides a way to compare samples of different thicknesses. The vertical axis is the effective modulus in Fig. 2(a) and the hardness in Fig. 2(b). By effective modulus, we mean that the measured modulus has contributions from the combination of the film and the substrate. These quantities are both functions of the load force. Note that at high loads (right half of the curves), all the measured curves (solid lines) tend to meet each other. This occurs because if the indenter is deeper, the silicon substrate dominantly contributes to the measured values. Thus, the data points in the low-load region (left half of curves) can better measure the film properties, since under these loads the effect of the substrate is minimal.¹⁴

The hardness and modulus data for each sample were averaged over the range of h between 1.2 and 2.0. The results are shown in Table II. It can be seen that all the Cs-implanted samples (samples 1, 2, and 3) show improved elastic modulus and hardness compared to sample A (uncured unimplanted). The more heavily doped samples show greater improvement, up to 56%, in both mechanical properties, especially after annealing. Furthermore, the annealed samples 2 and 3 exhibit a similar elastic modulus and hardness compared to sample B (UV-cured unimplanted).

Note that the above method reveals only the *relative* improvements of the mechanical properties from Cs-implantation and

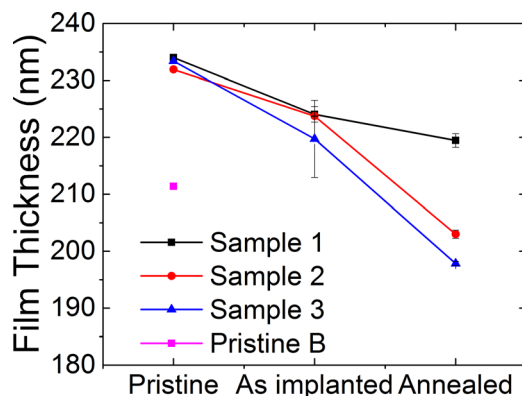


FIG. 1. Ellipsometry measured film thicknesses.

annealing. The true elastic modulus, which is an intrinsic property of the film itself, cannot be determined using this method.^{14–16} A possible technique to determine the absolute value of the elastic modulus is proposed here by utilizing a model developed by Stone.¹⁵ The model uses the substrate properties along with a range of possible absolute elastic moduli of the film to obtain a set of parametric curves. In Figure 2(a), the curves based on the Stone's model (hollow symbols) are plotted. In principle, by comparing the experimental curves in the low-load region to the parametric curves, one may determine the true elastic moduli of the film.¹⁴ However, because of the small thicknesses of the films, it was not possible to obtain sufficient data in the low-load region to determine the modulus directly. Thus, the averaging method described above was used to demonstrate the improvement of the *film* mechanical properties.

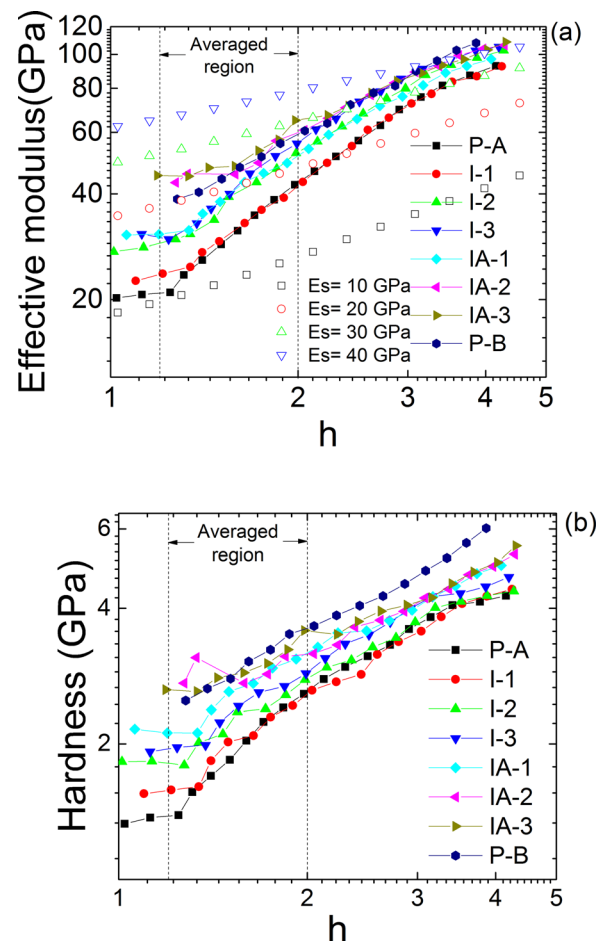


FIG. 2. Nano-indentation measured (a) effective modulus and (b) hardness. Simulation curves are also shown in (a) as hollow symbols. The sample legend is as follows: P-A—pristine uncured sample A and P-B—pristine UV-cured sample B. I-1, I-2, and I-3—implanted only samples and IA-1, IA-2, and IA-3 are implanted and annealed samples.

TABLE II. Averaged mechanical properties (data points that have $1.2 < h < 2.0$), and k -values. Sample labels: P-pristine, I-as implanted but not annealed, IA-implanted and annealed. Samples A, 1, 2, and 3 are uncured SiCOH films. Sample B is UV-cured SiCOH film.

Sample label	Averaged effective		Averaged hardness (GPa)	Relative change (%)	Normalized k -values	Relative change (%)
	modulus (GPa)	Relative change (%)				
P-A	33.6	N.A.	2.13	N.A.	3.2	N.A.
I-1	34.7	+3.04	2.22	+3.88	3.22	+0.47
I-2	41.1	+22.1	2.37	+11.0	3.75	+17.1
I-3	43.7	+29.9	2.46	+15.5	3.75	+17.1
IA-1	40.5	+20.3	2.64	+23.9	3.32	+3.76
IA-2	50.2	+49.1	2.95	+38.4	3.77	+17.8
IA-3	52.6	+56.5	3.02	+41.5	3.90	+22.0
P-B	46.3	N.A.	2.95	N.A.	3.2	N.A.

To understand the basis for these improvements, Fourier-Transform Infra-Red spectroscopy (FTIR) measurements were used to analyze the Si-O bond configuration in the film. The results are shown in Figure 3. The peak around 1140 cm^{-1} represents the Si-O-Si cage structure and the peak near 1065 cm^{-1} represents the Si-O-Si network structure.¹⁷ It can be seen that compared with Sample A (uncured unimplanted film), the Cs-implantation changes the majority of the Si-O-Si bonds from being a cage structure to a network structure. Higher Cs doses lead to a higher network-structure peak. This change contributes to the improvement of the mechanical properties.^{3,5}

To examine the electrical properties of these films, Capacitance-Voltage (C-V) measurements, utilizing a metal dot/dielectric/silicon structure and a pin-probe station, were performed to find the k -value of the samples. The setup details can be found in a previous publication.¹⁸ The measurement was carried out in ambient air and humidity. The results are also shown in Table II. It can be seen that all the implanted samples experienced an increase in k -values after implantation, and developed an even higher value after annealing.

According to the reported results^{3,5} for SiCOH dielectrics, carbon loss, especially Si-CH₃ bond loss, can lead to an increased k -value. This loss of Si-CH₃ bond is confirmed in this work with FTIR and X-ray Photoelectron Spectroscopy (XPS) depth profiles. The FTIR results are shown in Figure 4.

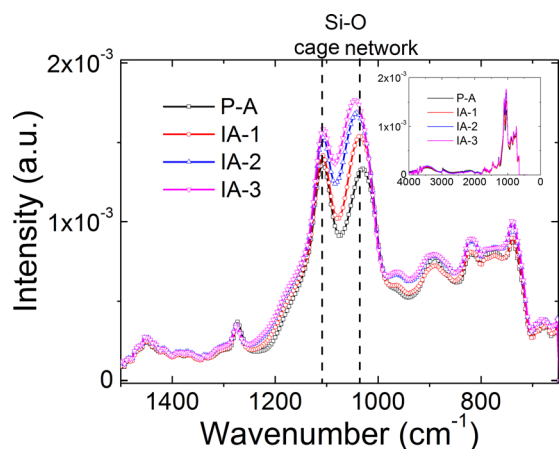


FIG. 3. FTIR measured Si-O bonds for type A films. The sample legend is as follows: P-A means pristine uncured sample A and IA-1, IA-2 and IA-3 are implanted and annealed samples.

The peak around 1274 cm^{-1} represents Si-CH₃ bonds.¹⁷ It can be seen that higher Cs doping leads to slightly lower levels of Si-CH₃ bonds. This is likely due to the fact that implanted Cs ions can break Si-CH₃ bonds during deceleration and thus cause carbon loss, since the Si-CH₃ bonds are much weaker than the Si-O bonds (4.7 eV vs 8.3 eV).⁵

The XPS depth profile results, e.g., comparisons between samples A, 3, and B are shown in Figure 5. It can be seen that the unimplanted samples A and B have constant atomic compositions through the entire depth of the film. Sample B shows a uniform carbon loss compared to sample A, because it has been UV-cured. In contrast, the as-implanted but not annealed sample 3 shows a carbon loss within the top half of the film. This can be attributed to the implanted Cs ions as described above. The implanted and annealed sample 3 shows additional carbon loss through the entire thickness of the film. This can be attributed to oxidation after the samples were removed from the annealing furnace. The inverse relationship between the oxygen and carbon XPS depth profiles indicates that oxygen atoms take the place of carbon atoms. Note that the extra oxygen can also explain the overall increase of the two Si-O-Si peaks shown in Figure 3. In Figure 5, by comparing as-implanted but not annealed sample 3 with sample B, it can be seen that Cs implantation and UV curing produce similar levels of overall carbon loss. Given the reasons for the two mechanisms of carbon loss in sample 3, it is reasonable to believe that reducing the implantation energy for thinner films than those used here while optimizing the annealing

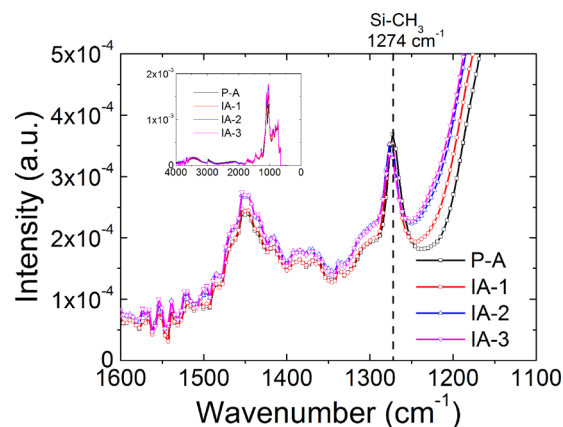


FIG. 4. FTIR measured Si-CH₃ bond for type A films. The sample legend is as follows: P-A means pristine uncured sample A and IA-1, IA-2 and IA-3 are implanted and annealed samples.

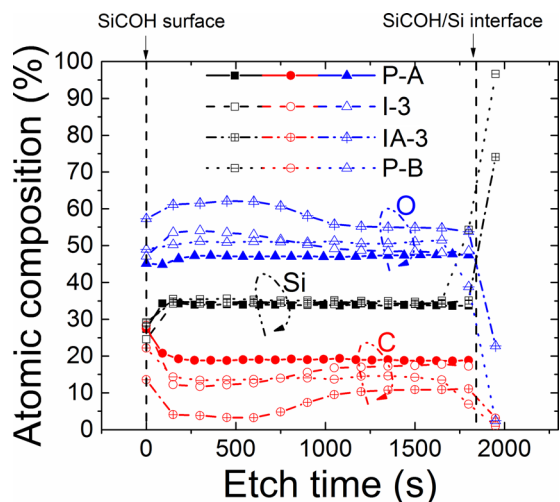


FIG. 5. XPS depth profiles for type A uncured films and the pristine UV-cured type B film.

conditions may also help to suppress both the carbon loss and the concomitant increase of the k -value.

Finally, time-zero dielectric breakdown (TZDB) characteristics were measured with the same system used for C-V measurements, except that the LCR meter was replaced with a picoammeter. Each sample was tested 20 times for 20 separate metal dots that were deposited on the sample. The box-plot¹⁹ statistics of the TZDB characteristics are shown in Fig. 6. It can be seen that for as-implanted samples, implanted Cs atoms did not cause significant degradation to the TZDB voltage. In fact, this may improve the TZDB voltage. Except for sample 3, it appears that the as implanted but unannealed samples have a higher TZDB voltage than the corresponding annealed samples and pristine samples A and B. Conversely, the implanted and annealed sample 3 shows a TZDB voltage higher than the as-implanted unannealed sample 3, as well as pristine samples A and B. The Cs ion has been shown to be relatively non-mobile in SiO₂ at temperatures lower than 800 °C.^{20,21} This may explain why the TZDB measurements do not degrade as the dose of implanted Cs ions increases.

In summary, the effects of dry Cs-ion implantation on the mechanical and electrical properties of uncured nonporous

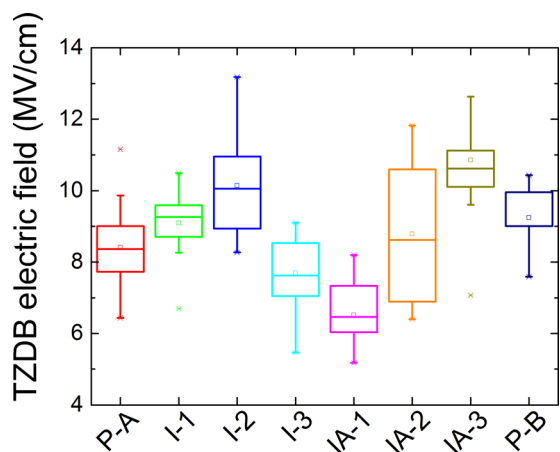


FIG. 6. TZDB box-plot statistics for type A uncured films and the pristine UV-cured type B film.

low- k SiCOH films have been investigated and compared with the UV-cured nonporous SiCOH film. The elastic modulus and hardness of the SiCOH films were found to improve with increasing Cs dose. This improvement is more significant for annealed samples. Two higher-dose samples show comparable elastic moduli and hardness to the UV-cured film. The improvement of the mechanical properties is attributed to an enhanced network structure of the Si-O-Si bonds. The k -values of the low- k films were found to increase gradually with dose after Cs implantation, and increase further after annealing. This increase is attributed to carbon loss in the film. Two mechanisms of carbon loss require optimization of implantation and annealing conditions. For low and medium Cs doses, the TZDB voltages of as-implanted but unannealed samples are actually higher compared with the pristine samples. However, for high Cs doses, an implanted and annealed sample shows a higher TZDB voltage than that for the pristine samples. Based on the above analysis, the medium or high Cs dose implantation has the potential to be a supplement to or substitution for the incumbent UV curing method in terms of improving the quality of the nonporous SiCOH film.

With the results shown above, it will be useful to extend this work to the PECVD deposited porous low- k films. Dynamic mode secondary-ion mass spectrometry may be used to detect Cs depth profile. Since UV-curing is currently used not only to strengthen mechanical properties but also to create pores in SiCOH films, we believe that Cs implantation should be investigated together with UV-curing on porogen-based films in the future.

The authors would like to thank J. E. Jakes for the helpful discussions about the nanoindentation experiments. This work was supported by the National Science Foundation under Grant No. CBET-1066231 and by the Semiconductor Research Corporation under Contract No. 2012-KJ-2359.

¹A. Grill, L. Perraud, V. Patel, C. Jahnke, and S. Cohen, in *The MRS Proceedings* (Cambridge University Press, 1999), p. 107.

²A. Grill, *Annu. Rev. Mater. Res.* **39**, 49 (2009).

³A. Grill, S. M. Gates, T. E. Ryan, S. V. Nguyen, and D. Priyadarshini, *Appl. Phys. Rev.* **1**, 011306 (2014).

⁴M. R. Baklanov and K. Maex, *Philos. Trans. R. Soc. A* **364**, 201 (2006).

⁵M. R. Baklanov, J. F. de Marneffe, D. Shamiryan, A. M. Urbanowicz, H. L. Shi, T. V. Rakhimova, H. Huang, and P. S. Ho, *J. Appl. Phys.* **113**, 041101 (2013).

⁶K. Lionti, W. Volksen, T. Magbitang, M. Darnon, and G. Dubois, *ECS J. Solid State Sci.* **4**, N3071 (2015).

⁷Y. Kayaba, K. Kohmura, H. Tanaka, Y. Seino, T. Odaira, F. Nishiyama, K. Kinoshita, S. Chikaki, and T. Kikkawa, *J. Electrochem. Soc.* **155**, G258 (2008).

⁸A. Zenasni, V. Jousseume, P. Holliger, L. Favennec, O. Gourhant, P. Maury, and G. Gerbaud, *J. Appl. Phys.* **102**, 094107 (2007).

⁹O. Gourhant, G. Gerbaud, A. Zenasni, L. Favennec, P. Gonon, and V. Jousseume, *J. Appl. Phys.* **108**, 124105 (2010).

¹⁰S. Nakao, J. Ushio, T. Ohno, T. Hamada, Y. Kamigaki, M. Kato, K. Yoneda, S. Kondo, and N. Kobayashi, in *Proceedings of the International Interconnect Technology Conference, Burlingame, CA, USA* (IEEE, 2006), p. 66.

¹¹A. M. Urbanowicz, K. Vanstreels, D. Shamiryan, S. De Gendt, and M. R. Baklanov, *Electrochem. and Solid-State Lett.* **12**, H292 (2009).

¹²R. S. Smith, T. Tsui, and P. S. Ho, *J. Electron. Mater.* **39**, 2337 (2010).

¹³J. F. Ziegler, M. D. Ziegler, and J. P. Biersack, *Nucl. Instrum. Methods B* **268**, 1818 (2010).

¹⁴X. Guo, J. E. Jakes, M. T. Nichols, S. Banna, Y. Nishi, and J. L. Shohet, *J. Appl. Phys.* **114**, 084103 (2013).

¹⁵D. S. Stone, *J. Mater. Res.* **13**, 3207 (1998).

- ¹⁶K. Vanstreels and A. Urbanowicz, *J. Vac. Sci. Technol. B* **28**, 173 (2010).
- ¹⁷A. Grill and D. A. Neumayer, *J. Appl. Phys.* **94**, 6697 (2003).
- ¹⁸D. Pei, M. T. Nichols, S. W. King, J. S. Clarke, Y. Nishi, and J. L. Shohet, *J. Vac. Sci. Technol. A* **32**, 051509 (2014).
- ¹⁹N. J. Salkind and K. Rasmussen, *Encyclopedia of Measurement and Statistics* (SAGE Publications, Thousand Oaks, California, 2007).
- ²⁰A. Hurrell and G. Sixt, *Appl. Phys.* **8**, 293 (1975).
- ²¹C. L. Schutte and G. M. Whitesides, *Chem. Mater.* **2**, 576 (1990).